UTILIZING NASA SATELLITE MISSIONS TO IDENTIFY BARK BEETLE INFESTATION IN SEQUOIA NATIONAL PARK

Michelle E. Newcomer, San Francisco State University
Janine E. Bird, San Jose State University
Shaina M. Sabatine, Colorado State University
Gabriel C. Sady, UC Santa Cruz
Ashley M. Stalzer, UC Santa Cruz
Tim A. Wheeler, UC San Diego

Science Advisor
Cindy Schmidt, UC Santa Cruz, San Jose State University
Science Mentor
J. W. Skiles, Ph.D., NASA Ames Research Center

DEVELOP NASA Ames Research Center
M.S. 242-4
Moffett Field, California 94035
MichelleNewcomer@hotmail.com
Joseph.W.Skiles@nasa.gov

ABSTRACT

Bark beetle-induced tree mortality has increased over the last few decades, exacerbated by below-average precipitation and a loss of soil nutrients, forcing park managers to improve bark beetle monitoring techniques. Bark beetle dynamics were investigated during summer 2009 at 32 sites within Sequoia National Park, California with the aim of correlating field data with satellite imagery to provide forest managers with a more efficient methodology for tracking, monitoring, and forecasting bark beetle outbreaks. Field parameters included visual assessments of the presence and degree of bark beetle-induced mortality and percent canopy cover. Ancillary data such as relative leaf chlorophyll concentration and soil nutrient concentrations including sodium [Na^+], nitrate [NO_3^-], and potassium [K^+] were collected for each 15 × 15 meter site. The relationship between bark beetle attacks and potassium [K^+] shows higher concentrations of that nutrient in areas with healthy trees. Additionally, algorithms from three satellites were used to identify areas of moisture and vegetation stress; including the Ratio Vegetation Index (RVI) from ASTER, Enhanced Wetness Difference Index (EWDI) from Landsat Thematic Mapper (TM5), Disturbance Index (DI) from MODIS, and four other vegetation indices from Landsat TM5. Vegetation indices show uniform vegetation stress across various years.

INTRODUCTION

Bark beetles, specifically the fir engraver *Scolytus ventralis*, the mountain pine beetle *Dendroctonus ponderosae*, and the western pine beetle *D. brevicomis*, have spread rapidly over the last several years due to a combination of warmer climate and drought (Carroll *et al*., 2004; Safranyik and Carroll, 2006). Temperature driven stresses contribute to die-back during normal periods of drought, increasing the vulnerability of trees to many different sources of mortality (Van Mantgem and Stephenson, 2007). In addition, historical fire-suppression has increased the availability of suitable host trees (Carroll *et al.*, 2004; Safranyik and Carroll, 2006). Bark beetles naturally thrive on stressed trees, removing those struck by drought or other disturbances (Samman and Logan, 2000). However, increasing bark beetle populations allow for attacks on otherwise healthy trees, destroying far more than is typical (Westfall, 2005). In a 60-year mapping analysis of vegetation and landscape change in the Sierra Nevada, Thorne *et al.,* (2008) identified elevation-dependant vegetation changes. They found that at lower elevations, pines and oaks were being replaced by annual grasslands, whereas at higher elevations, the pines were being replaced by Montane Hardwood which is a transition conifer/broadleaf mix (Thorne *et al.,* 2008). This vegetation shift reflects new climatic and disturbance scenarios where vegetation re-establishment conditions increase the probability for other disturbances because of the time required for regeneration (Thorne *et al.,* 2008).

Current methods for monitoring bark beetle infestation and forest disturbance include aerial detection surveys, remote sensing techniques, and ground surveys (USDA). The USDA Forest Service has provided aerial detection surveys every year beginning in 1993, allowing monitoring of bark beetle infestation (USDA). The cost and time of aerial and ground surveys creates a demand for a more efficient means of detecting bark beetle damage for the National Park Service. Fortunately, remote sensing methods can assess the location of bark-beetle damage by identifying the red-attack stage of infestation using vegetation specific wavelengths (discussed below) (Wulder *et al*., 2006).

Remote sensing techniques for infestation detection yield highest correlations when bark beetles manifest in homogeneous pockets of mortality (Healy *et al.,* 2005), characteristic of remote sensing studies in British Columbia, Canada, and other prominent mortality zones (Wulder *et al*., 2006, Hais *et al.,* 2009, Skakun *et al*., 2003, Jin and Sader, 2005). However, in Sequoia National Park, California, ground truthing shows that the diversity of trees may abate total destruction. The intermixing of healthy and unhealthy trees makes aerial detection surveys less accurate, and creates difficulty when using remote sensing to differentiate between classes. Despite the appearance of relatively healthy stands, bark beetles are a large scale problem, infecting 9.4 million acres across the U.S. in 2008, and with lengthening summer droughts, this trend is expected to continue (USDA).

This projects aims to identify individual bark-beetle infested trees and areas of possible future risk among the heterogeneous red-attack stands using three remote sensing measures calibrated with field measurements. Goals also include determining differences between mortality and non-mortality sites when analyzing various measures of forest health. Thirty-two (32) field sites were sampled and used to calibrate the Ratio Vegetation Index (RVI) from the ASTER sensor on the NASA Terra Satellite, the Enhanced Wetness Difference Index (EWDI) from Landsat TM5, and the Disturbance Index (DI) from MODIS on the NASA Aqua Satellite. Other vegetation indices used include, NDMI, NDVI, DI, and DI', calculated using Landsat Thematic Mapper 5 (TM5) (Table 1).

Table 1. Satellite indices used to map stress in Sequoia National Park.

Satellite Indices					
Abbreviation	**Name**	**Index**	**Satellite / Sensor**	**Description**	**Reference**
EWDI	Enhanced Wetness Difference Index	$EWDI = TC3(2007) - TC3(2008)$	Landsat	water stress	Skakun *et al*., 2003
NDVI	Normalized Difference Vegetation Index	$NDVI = \frac{(NIR - RED)}{(NIR + RED)}$	Landsat	vegetation stress	Rouse *et al*., 1974
NDMI	Normalized Difference Moisture Index	$NDMI = \frac{NIR - SWIR}{NIR + SWIR}$	Landsat	vegetation & water stresses	Jin and Sader, 2005
Landsat DI	Landsat Disturbance Index	$DI = Brightness - (Greeness + Wetness)$	Landsat	tasseled cap based disturbance	Healey *et al*., 2005
Landsat DI'	Landsat Disturbance Index'	$DI' = Wetness - Brightness$	Landsat	tasseled cap based disturbance	Hais *et al*., 2009
MODIS DI	Disturbance Index	$DI_{LST/EVI} = \frac{LST_{\max} / EVI_{\max}}{LST_{\bar{x}\max} / EVI_{\bar{x}\max}}$	Terra & Aqua / MODIS	vegetation & temperature stresses	Mildrexler *et al*., 2007
RVI	Ratio Vegetation Index	$RVI = \frac{NIR}{Red}$	Terra / ASTER	vegetation stress	Elvidge and Chen, 1995

Bark Beetle Phenology

Healthy trees provide the most abundant food source for bark beetles, but are also most resistant to beetle infestation, as they defend against bark beetle attack by producing abundant amounts of resin laden with insecticidal and fungicidal compounds. A tree that is drought-stressed is unable to produce enough resin to combat bark beetles therefore beetles are most successful when they find trees that have undergone sudden and severe moisture stress (DeMars and Roettgering, 1982).

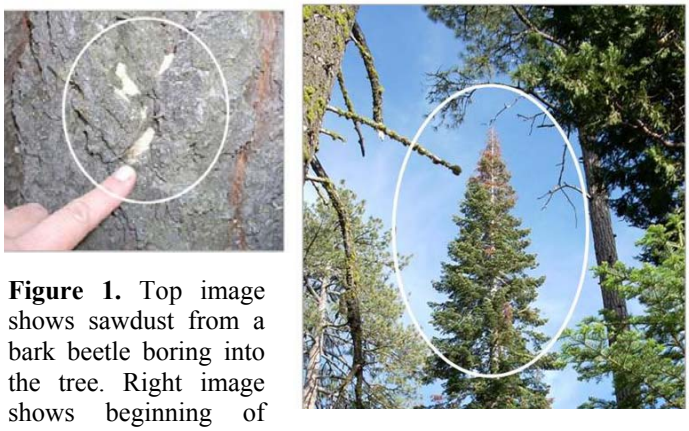

Figure 1. Top image shows sawdust from a bark beetle boring into the tree. Right image shows beginning of red-attack stage.

Generally in late summer swarms of adult bark beetles invade and collectively overpower the host tree's defenses (Safranyik *et al*., 1974). The beetles introduce spores of blue stain fungi, such as *Ophiostoma clavigerum* and *O. montium* into the tree's inner bark, further harming the tree's vascular system (Ballard *et al*., 1982). Female bark beetles bore through the outer bark, leaving sawdust or resin as evidence of the attack. Eggs mature within a year (Amman and Cole, 1983).

Infested trees undergo a three-stage process during bark beetle infestation. The first stage, green attack, has no visual signs at the canopy level, and is therefore extremely difficult to detect via remote sensing (Reid, 1961). This is the initial onset where the beetles bore into the tree and infest the phloem (Henigman *et al*., 1999). Consequently, the tree slowly loses nutrients and has roughly a year before it transitions into the red attack stage (Hill *et al*., 1967).

The red attack stage is visible to sensors, occurring as beetle larvae feed on the tree's phloem (Carroll and Safranyik, 2004). The crown turns an iconic red color as water and nutrients cease to flow upwards from the roots causing pigmentation to break down and mortality to progress (Figure 1: Hill *et al*., 1967, Safranyik *et al*., 1974). The final stage of attack is gray attack, named after the ashen appearance of the tree. Here the tree has lost all foliage and is biologically dead (British Columbia Ministry of Forests, 1995). Outbreaks can decimate a forest leaving thousands of standing dead trees as in the extreme outbreaks are occurring in western forests.

Study Area

All field sites were located within Sequoia National Park, CA, within a 5 km radius at 36.604 latitude and at 118.787 longitude. The park is located east of the San Joaquin Valley, at the southern end of the Sierra Nevada mountain range (Figure 2). Vegetation consists of montane forest with lodgepole, ponderosa, and jeffrey pines; white and red fir; and sequoia trees at higher altitudes. Lower elevations include a large amount of understory vegetation mixed among the trees. Topographic complexity and a Mediterranean climate zone contribute to the variability in average annual precipitation. Temperature and precipitation conditions consist of cold wet winters and warm dry summers, as well as high summer transpiration rates. Drought and fire are recurring events in the Southern Sierras, and are important ecological processes that affect species composition and forest structure. Before 1900, stand densities consisted of 100-200 stems ha^{-1} whereas today stem density is found to exceed 500 stems ha^{-1}; a change known to have implications on the natural fire cycle (Kilgore, 1973). Fire suppression regimes beginning in 1900 demonstrate the susceptibility of forest stands to changes in ecological processes, jeopardizing the ability of the forest to resist disease and insect infections (Minnich and Padgett, 2003).

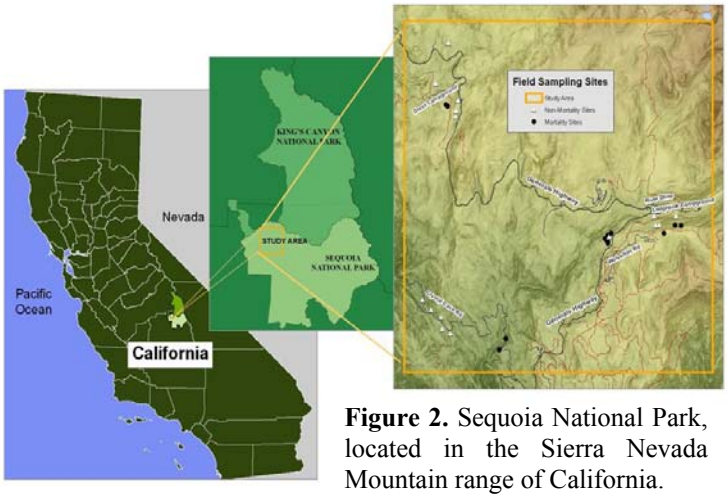

Figure 2. Sequoia National Park, located in the Sierra Nevada Mountain range of California.

METHODOLOGY

Site Selection Process

Site selection was based on GIS data from the USDA Forest Service (USDA, 2009) and National Park Service (NPS, 2009). Shape-files of the Sequoia National Park boundary, local vegetation communities, USDA FS aerial detection surveys of forest disturbance and bark beetle mortality, roads, and a 10 m Digital Elevation Model (DEM) were used. To generate random points, ArcMap 9.3 was used to create two sets of random sampling points within a 500 m road buffer; one set within bark beetle mortality polygons, and one set within pine and fir tree communities where canopy cover was ≥ 70% and bark beetles were not present based on the aerial detection survey. Each generated point was moved to the center of a 15 × 15 m ASTER satellite pixel to directly relate the *in-situ* data with satellite imagery. Several sites included rock outcroppings or small streams, and in these cases the plot was relocated by 15 m at a random bearing. Often the random mortality sites contained generous amounts of healthy trees therefore several sites were relocated to the closest red-attack tree. A total of 32 sites were sampled.

Field Data

Soil samples were taken in the center of each 15 × 15 m site from the first twenty (20) centimeters of soil below the duff. The samples were sifted through a 0.295 mm mesh screen and stored for *ex-situ* analyses (sodium and potassium concentrations). Soil nitrate was measured at camp twenty four (24) hours later using a Cardy Nitrate Meter. Soil samples were warmed in a solar oven over the course of a day, and any residual moisture was removed by heating the soil over a camp stove, as moisture skews results. Soil methodology was taken from D'Antoni *et al*., (2007). Soil moisture readings were taken adjacent to the soil sample hole using a Fieldscout TDR 100 moisture meter with 20 cm rods. The genus, health, and quantity of all pine and fir trees within the 15 × 15 m plot were recorded; health was classified as green (no signs of bark beetle attack), red (visible red foliage and bark beetle boring holes in trunk), or gray (defoliated and dead from bark beetle attack).

Chlorophyll data were taken from the tree nearest to the center of each plot. Only firs and pines ≥ 1 m in height were sampled. Relative chlorophyll measurements were taken from tree needles using a Fieldscout CM 1000 chlorophyll meter, which generates a relative greenness index. Red and gray trees were analyzed together as 'mortality trees' for chlorophyll, and compared with green, healthy trees that were considered 'non-mortality.' Percent canopy cover was estimated and classified as 0-5%, 5-10%, 10-25%, 25-50%, 50-75%, or 75-100%.

Statistical Analyses

Paired Student's t-tests were used to test for significant differences between mortality and non-mortality sites in percent canopy cover, soil moisture and nutrients (nitrate, potassium, and sodium), leaf chlorophyll measurements, ASTER RVI values, MODIS DI, and Landsat vegetation index yearly averages. Differences were considered significant where $p \leq 0.1$ or marginally significant where $p < 0.2$.

Satellite Image Processing

Past research has utilized various ratios of satellite spectral bands and other algorithms to detect bark beetle infestation in areas of intense mortality (Healey *et al*., 2005, Hais *et al.,* 2009, Jin and Sader, 2005, Franklin *et al*., 2000, Skakun *et al*., 2003). This study aims to accomplish the same in Sequoia National Park where bark beetle infestation is present, but not in large homogeneous patches such as those found in Colorado and Canada.

Landsat TM5. Landsat TM5 has 30 meter spatial resolution and 7 bands spanning the visible and thermal portions of the electromagnetic spectrum. Twelve cloud free images were downloaded from GLOVIS (http://glovis.usgs.gov/) for June, July, and August from 2002 to 2008. Each image was radiometrically corrected using ERDAS 9.3 and then transformed into reflectance values using the method from Chander and Markham, (2003). Five indices were used; the Enhanced Wetness Difference Index (EWDI), the Normalized Difference Vegetation Index (NDVI), the Normalized Difference Moisture Index (NDMI), and two different Disturbance Indices (DI and DI') were calculated.

The *tasseled cap*, or *Kauth-Thomas transformation*, is a widely used vegetation index and shows three axes of vegetation: brightness, greenness, and wetness (Crist and Kauth, 1986). The EWDI differences the wetness layer from two *tasseled cap* images to detect water stress (Equation 1; Skakun *et al.,* 2003) where Wetness (2007) is the wetness layer from the first year and Wetness (2008) is for the second year.

$$EWDI = Wetness(2007) - Wetness(2008) \qquad \text{(Equation 1)}$$

EWDIs were computed in ERDAS 9.3 for June 2006-2007, 2007-2008; July 2007-2008, 2008-2009; and August 2005-2006, 2006-2007, 2007-2008. The EWDIs for July and August were uploaded into ArcMap 9.3. The EWDI pixel and 3x3 pixel area (8100m^2) reflectance values corresponding to each field site were obtained (Figure 3). The values for mortality and non-mortality sites were averaged for each month and statistical significance between site classes was computed in SPSS for each month and year (Appendix A).

The Normalized Difference Vegetation Index (NDVI) and the Normalized Difference Moisture Index (NDMI) were computed in ERDAS Imagine 9.3 (Equations 2 and 3) and data values for pixel and 3x3 pixel areas extracted in ArcMap 9.3 to detect differences in vegetation between site classes from August 2003 through August 2008. Additionally, NDMI averages were computed for small (≤ 20 Landsat pixels) versus large polygons, as discussed in ASTER methods. Both NDVI and NDMI detect vegetation change, but the NDMI better assesses water and vegetation stress for conifers (Jackson *et al*., 2004). The NDMI quantifies the spectral contrast between near (NIR) and short wave infrared (SWIR) wavelengths whereas the NDVI ratios the differences between the NIR and RED portions of the spectrum. NDMI values decrease as bark beetles infest the forest because conifer foliage degrades leading to declined NIR reflectance values but greater SWIR values due to increased exposure of soils to the satellite (Hais *et al*., 2009).

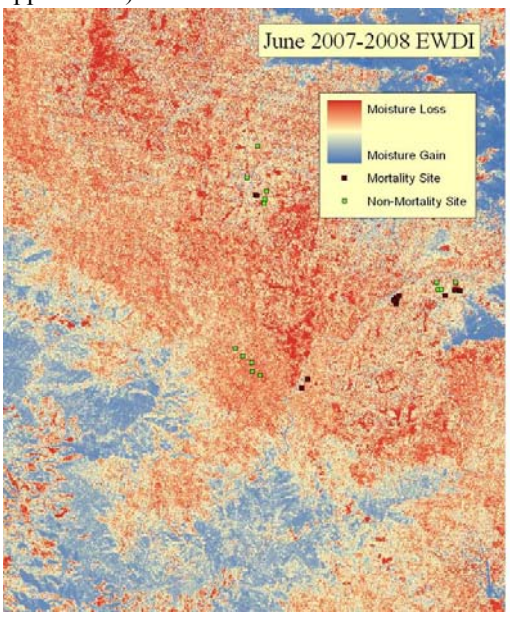

Figure 3. Enhanced Wetness Difference Index shows decreased moisture within our mortality and non-mortality field sites.

$$NDMI = \frac{(NIR - SWIR)}{(NIR + SWIR)} \qquad \text{(Equation 2)}$$

$$NDVI = \frac{(NIR - RED)}{(NIR + RED)} \qquad \text{(Equation 3)}$$

Finally, two different Disturbance Indices were analyzed from single date *tasseled cap* images to measure vegetation degradation. Similar to other vegetation indices, both reliably detect disturbance when there is excellent spectral contrast between healthy and unhealthy forested stands (Healey *et al.,* 2005). The first disturbance index (Equation 4) highlights the contrast between healthy forest stands and bare ground (Healey *et al.,* 2005). This equation is more appropriate for fire-damaged forests where understory vegetation is completely removed and soil reflects high brightness values. However, bark beetles do not remove understory vegetation; therefore Hais *et al*. (2009) modified the DI into DI' (Equation 5) to more appropriately account for bark beetle disturbance.

$$DI = Brightness - (Greeness + Wetness) \qquad \text{(Equation 4)}$$

$$DI' = Wetness - Brightness \qquad \text{(Equation 5)}$$

DI' was then compared to the MODIS DI image (discussed below) by calculating root mean square error Also, aggregated snowfall and precipitation data from January to August for each year from 2002-2008 was obtained (Desert Research Institute) and compared to the average DI' in the Mortality and Non-Mortality sites for each year. Finally, additive Color Logic maps were generated from DI' to visually analyze disturbance over time. All the statistical analyses and comparisons with the Landsat DI' are discussed in the Results section.

ASTER. Two ASTER images (from June 2007 and August 2008) were downloaded from the online Warehouse Inventory Search Tool (WIST) website (https://wist.echo.nasa.gov/~wist/api/imswelcome/). Level 2 surface reflectance image products were used to calculate and investigate changes in vegetation stress between the two years using the Ratio Vegetation Index (RVI) (Equation 6) (Elvidge *et al.,* 1995).

$$RVI = \frac{NIR}{Red} \qquad \text{(Equation 6)}$$

As vegetation becomes increasingly stressed, it reflects progressively less near infrared (NIR) radiation but more Red electromagnetic radiation, thus the RVI will decrease with escalating stress (Short, 2005). Since bark beetles thrive on stressed trees, confirmation of stress in the USFS Aerial Detection Survey polygons can help validate the presence of bark beetle attack.

The two ASTER images were geo-rectified to a geometrically accurate Landsat image using several ground control points. Raster files containing the RVI were created for each year using the two corrected ASTER images. An image of the percent change of RVI in Sequoia National Park between 2007 and 2008 was then created (Figure 4a). Thirty-one polygons retrieved from the US Forest Service aerial detection surveys of bark beetle attack were identified in the park. Polygons were divided into two groups by size. "Small" polygons were defined as polygons containing ≤ 20 ASTER pixels (≤ 4500 m^2), and "Large" polygons were defined as polygons containing greater than 20 pixels. Average percent change in RVI for each polygon as well as minimum and maximum values were recorded for analysis. The minimum and maximum values were used to find common RVI percent change values between polygons. These common values were utilized as threshold numbers and defined as the range in which minimal stress occurs in this forest. Values above the threshold were identified as stressed and values below the threshold were identified as healthy. A map showing these three zones was created to show an overall picture of stress (Figure 4a). These red areas may indicate the direction of possible bark beetle spread.

MODIS. MODIS data were obtained from the United States Geological Survey (USGS) website (https://lpdaac.usgs.gov/). Twelve images per year from the MODIS Aqua satellite beginning in 2002 up until 2008 were used for this study. Both land surface temperature (LST) and enhanced vegetation index (EVI) were used to compile the disturbance index (DI) (Equation 7), as described in Mildrexler *et al*. (2007).

$$DI_{LST/EVI} = \frac{LST_{\max} / EVI_{\max}}{LST_{\bar{x}\max} / EVI_{\bar{x}\max}} \qquad \text{(Equation 7)}$$

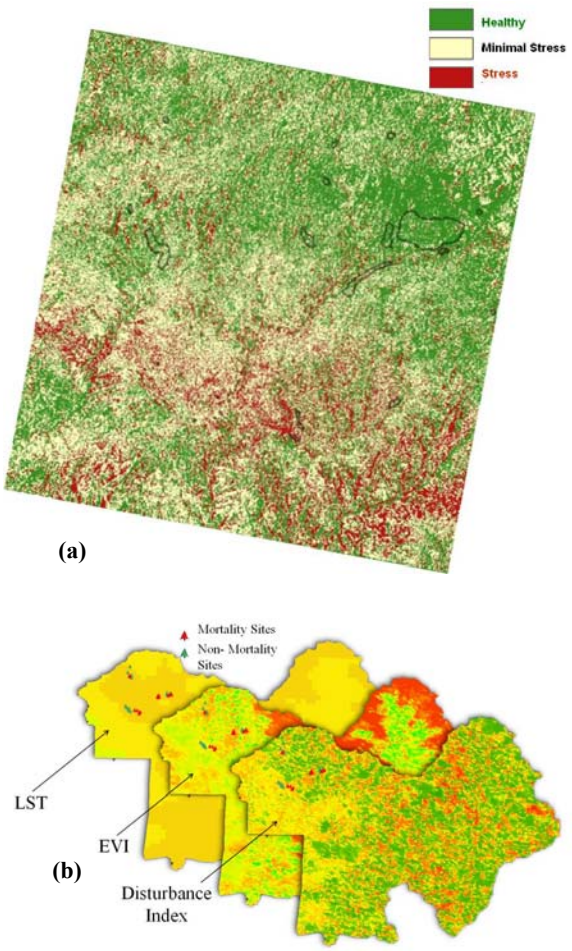

Figure 4. (a) ASTER RVI Map of healthy and stressed areas of Sequoia National Park calculated between June 2007 and August 2008. NFS aerial survey polygons are outlined in black**. (b)** MODIS Disturbance Index calculation method.

An ecological disturbance is a sustained disruption of natural forest functions, and includes disturbance from fires, drought, and insect defoliation (Mildrexler *et al*, 2007). Disturbance events change the energy balance at the site, and including the MODIS LST product in the DI algorithm estimates the dynamic energy exchanges occurring across the spatial landscape (Mildrexler *et al*., 2007). EVI (Equation 8) is essentially a modified NDVI where NIR, RED, and BLUE are the near-infrared, red, and blue wavelengths respectively. L is a soil adjustment factor, C_1 and C_2 are coefficients used to correct for aerosol scattering. Usually L=1, G = 2.5 C_1=6.0, and C_2=7.5. EVI shows sensitivity to high biomass regions; however it also shows considerable noise under vast terrain changes (Matsushita *et al*., 2007). The MODIS DI is very effective at identifying disturbance when both LST and EVI contribute anomalies to the signal, and as more yearly mean-maximum values are contributed to the scene in the denominator, the index better represents the undisturbed baseline in which to assess an anomaly (Mildrexler *et al*, 2007). EVI is defined as (Matsushita *et al*, 2007):

$$EVI = G * \frac{NIR - RED}{NIR + (C_1 * RED - C_2 * BLUE) + L} \qquad \text{(Equation 8)}$$

Each image was imported into ERDAS Imagine. Twelve images per year spanning seven years produced yearly maximum images for LST and EVI. An LST and EVI multiyear mean was subsequently computed from these images. All images were then reprojected and resampled into the UTM WGS 84 North, Zone 10 coordinate system. The finished images were used to calculate the yearly DI final image (Figure 4b). The same polygons as used in ASTER processing were compared across all seven years of the MODIS disturbance index. Polygons were already classified by size during the ASTER analyses. However, the large pixel sizes of the MODIS images caused small polygons to take up ten percent of a pixel's area. For polygons embedded in a single pixel, only that pixel's value was chosen to represent that polygon. For polygons centered on many pixels, the average value was taken. The largest polygons spanned multiple pixels, for which all pixels with > 50 % coverage were averaged.

RESULTS

Field Measurements

Percent canopy cover was higher in non-mortality sites, although the difference was not significant at the 0.1 level ($t = 1.51$, $p = 0.14$). Soil moisture, measured as percent volumetric water content, did not differ between mortality and non-mortality sites ($t = 0.98$, $p = 0.33$). Nitrate and sodium were not significantly different between site classes ($t = 0.25$, $p = 0.80$; $t = 0.25$, $p = 0.81$, respectively). Potassium was significantly higher in non-mortality sites ($t = 1.95$, $p = 0.06$). Relative chlorophyll measurements were also significantly higher for green trees than for red trees that had been killed by bark beetles ($t = 6.59$, $p < 0.0001$). Results are shown in Table 2.

Table 2: Percent canopy cover, soil moisture (percent volumetric water content), soil nitrate (NO_3-), soil potassium (K+), soil sodium (Na+), and relative leaf chlorophyll content (0-999 index). Means ± 1 SD. Values with b superscript are significantly different.

	Site Statistics					
Site Class	% Canopy Cover	Soil H_2O (% VWC)	NO_3^- ppm	K^+ ppm	Na^+ ppm	Chlorophyll Index
Mortality	37.14 ± 20.43^a	4.6 ± 2.5^a	8.3 ± 4.4^a	46.07 ± 25.60^a	129.33 ± 40.44^a	82.31 ± 9.56^a
Non-Mortality	52.14 ± 31.07^a	3.6 ± 3.3^a	7.9 ± 4.3^a	77.40 ± 65.19^b	132.67 ± 33.69^a	162.32 ± 45.68^b

Satellite Data

ASTER. ASTER RVI analyses showed significantly higher stress in small (≤ 4500 m^2) visually-detected bark beetle polygons versus larger ones ($t = 4.09$, $p = 0.0003$). This, along with visual assessments of the polygons, suggests a loss of accuracy in the aerial bark beetle mortality detection methodology with increasing polygon size (Figure 5a). Since polygons were all defined as 'bark beetle mortality' areas, it was expected that the average percent change in RVI between 2007 and 2008 be similar between all the polygons regardless of size, and that their magnitudes be in the stressed range. However, this was not the case (Figure 5b). Ground truthing of the mortality polygons in Sequoia National Park indicated a large interspersing of healthy green trees among red attack trees. This information is important when validating bark beetle mortality polygons labeled by the NFS through aerial detection surveys.

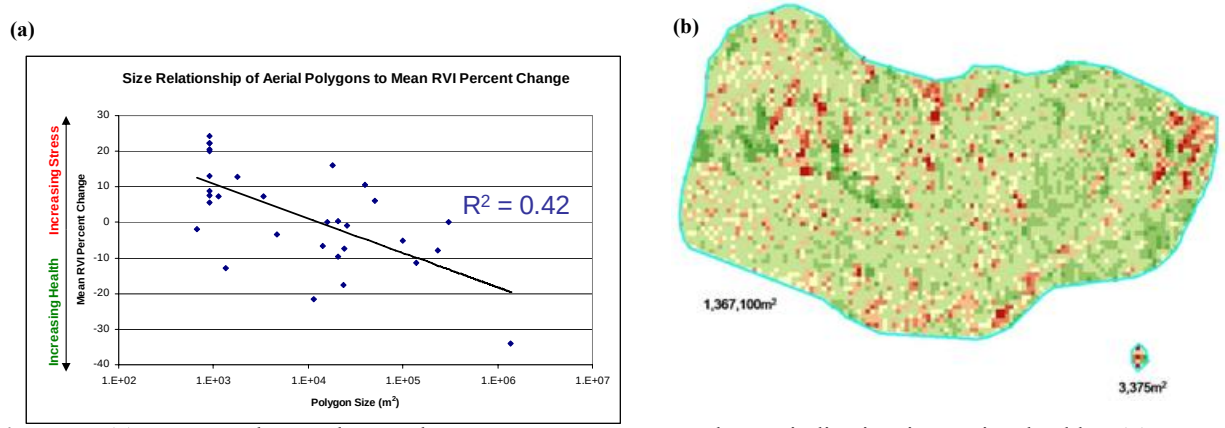

Figure 5. (a) Larger polygons have a lower mean RVI percent change indicating increasing health. **(b)** Larger aerial detection polygons incorporate healthy and dead trees, while smaller polygons more accurately represent dead areas.

Landsat TM5. The four indices; EWDI, NDVI, NDMI, and DI were used to generate 41 queries of significance between site classes. Queries showed 3/22 comparisons were marginally significant between site classes (Appendix A). Yet, the NDMI showed significantly higher values in small aerial detection survey polygons rather than larger ($t = 1.69$, $p = 0.10$) and between site classes (Figure 6a). With only 1/22 queries giving significance, visual analysis of each index proved more insightful.

First, the EWDI showed cyclical moisture patterns. For example, 2006-2007 showed increased wetness, and 2007-2008 showed decreased wetness throughout the forested areas. However, this contradicts data reporting opposite patterns for rain and snowfall (Table 3). This may happen because precipitation and snowfall data were taken at a single site, and therefore may be an inaccurate representation of rain and snowfall patterns for that year (Desert Research Institute). Second, the NDMI showed similar results to the NDVI. Although insignificant, when plotted against time, non-mortality sites displayed higher NDMI values than mortality (Figure 6a).

Third, Landsat DI' and MODIS DI show consistency with a root mean square error of 22.6%, and both demonstrate the oscillations from 2005-2008 that may be attributed to precipitation and snowfall. There was a negative relationship between DI' and both snowfall and precipitation with R^2 values of 0.77 and 0.71 respectively (Figure 6b), with the interpretation that as moisture deposition increases, the DI' value decreases indicating less disturbance. Finally, the additive color logic map for the DI' showed landscape change from 2002-2005-2008 and is useful for forest managers to detect disturbed regions that have yet to recover (Figure 7).

MODIS. The MODIS Disturbance Index was analyzed over seven years and showed significant differences in four of those years. Years 2002-2004 were not significantly different between mortality and non-mortality sites. In 2005 and 2006 the non-mortality sites showed significantly higher levels of disturbance than mortality sites ($t = 1.68$, $p = 0.10$; $t = 2.66$, $p = 0.01$, respectively). In 2007 and 2008 the reverse trend was seen, and mortality sites showed higher levels of disturbance than non-mortality sites (Table 4; $t = -1.89$, $p = 0.07$; $t = -2.57$, $p = 0.02$, respectively).

The MODIS DI shows a trend between site classes, where for two years (2005-2006) overall disturbance levels decreased across the landscape, while non-mortality site disturbance levels remained significantly higher than mortality sites. The following two years (2007-2008) exhibit an overall increase in disturbance and mortality sites begin to show significantly *higher* disturbance levels compared with non-mortality sites.

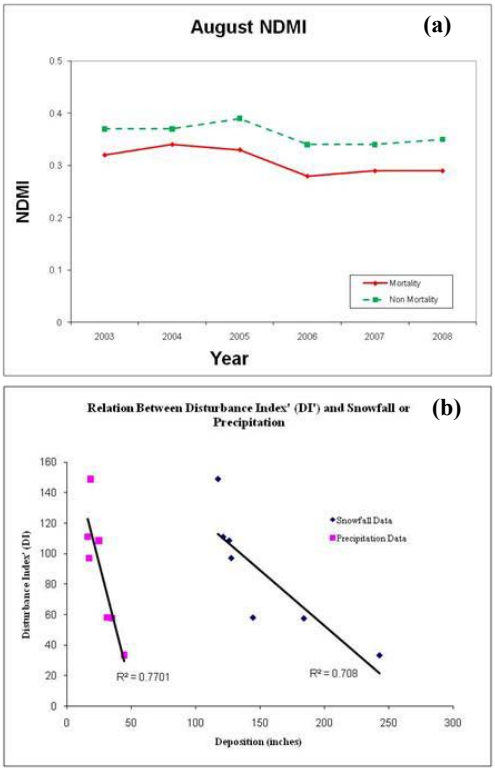

Figure 6. (a) Landsat shows higher average August NDMI values for non-mortality sites than mortality for each year; however this difference is not significant. **(b)** There is a negative relationship between DI' and snowfall or precipitation for years 2002-2008 implying decreasing disturbance with increasing moisture deposition.

Table 3: Landsat meteorological trends over two years.

	Summer 2006-2007	Summer 2007-2008
EWDI	↑	↓
DI' *	↑	↓
Rain and Snow **	↓	↑

*DI incorporates an average of June, July, and August

** Rain and Snow represent aggregated totals from January to August

Table 4: MODIS Disturbance index values. Means ± 1 SD. Values with b superscript are significantly different.

	MODIS Disturbance Index						
Site Class	2002	2003	2004	2005	2006	2007	2008
Mortality	0.94 ± 0.19^a	1.07 ± 0.16^a	1.06 ± 0.09^a	0.97 ± 0.14^a	0.81 ± 0.11^a	1.28 ± 0.13^a	1.14 ± 0.13^a
Non-Mortality	0.97 ± 0.13^a	1.02 ± 0.09^a	1.01 ± 0.09^a	1.05 ± 0.10^b	0.93 ± 0.15^b	1.16 ± 0.18^b	1.00 ± 0.16^b

DISCUSSION

Soil nutrients may have an influence on bark beetle infestation, and significantly higher levels of potassium in non-mortality sites found in this study warrant further research. Concentrations of soil potassium are important for regulating water use by the plant and may therefore play a role in the breakdown of a plant's health during drought (Samuel Roberts Foundation, 2004). Potassium controls osmo-regulation, stomatal function, enzyme activation, and when quantities are limited, decreases the rate of photosynthesis within the tree (Ericsson and Kähr, 1993). In a study on the effects of fire on cheatgrass in ponderosa pine forests, exchangeable soil potassium levels increased from 137 ppm before the fire to 150 ppm after (Keeley and McGinnis, 2007). In Sequoia National Forest, potassium concentrations may be highly influenced by fire cycles. Depressed nutrient cycles from decades of fire suppression may have an impact on the susceptibility of a forest to bark beetle infestation.

The USFS aerial detection survey is excessively generalized for fieldwork purposes. The polygons visited contained trees in the red attack stage, but the area identified by the USFS as having mortality was much larger than the spatial extent of actual tree mortality. Additionally, ASTER, Landsat TM5, and MODIS all showed higher accuracy in smaller aerial detection polygons rather than larger due to the high spatial heterogeneity that bark beetles exhibit. For ASTER, the high spatial heterogeneity in which bark beetles infest in the field causes intermingling of green trees with red trees. This causes high heterogeneity and skews the average RVI value for large polygons in the healthier direction. For Landsat, larger polygons contain a mixture of soil and other materials that bring down the NDMI value because of the higher SWIR reflectance of soil and in stands of healthy trees (*Hais et al*., 2009). Therefore, defining large areas in Sequoia National Park as containing a majority of bark beetle mortality inaccurately represents the degree of infestation, and consequentially over-represents the area encompassed by bark beetle infestation. Present bark beetle conditions in Sequoia National Park require aerial detection surveys to focus on small, homogeneous regions rather than broad, expansive areas.

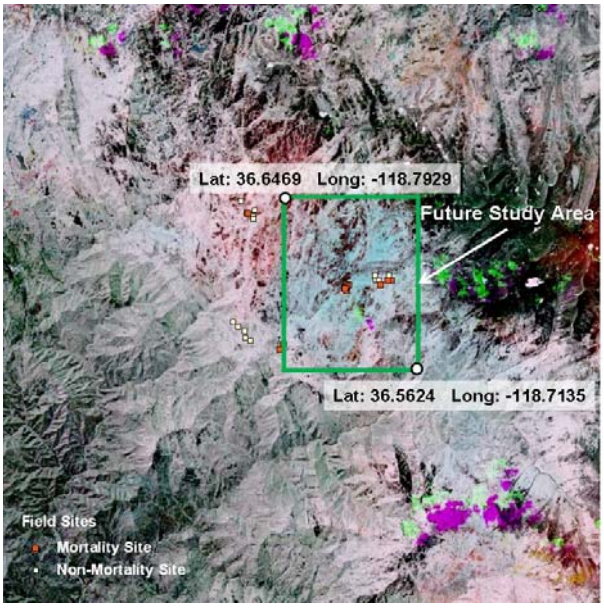

Figure 7. The DI' additive color logic map shows landscape change from 2002-2005-2008. The 2002 image is loaded through the red gun, the 2005 through the green, and the 2008 through the blue. Red indicates a disturbed region before 2002 that has recovered by 2005. Cyan implies forest disturbance between 2002-2005 that has not yet recovered in 2008. Green shows landscape disturbance between 2002-2005 that recovered by 2008. The purple shows increasing landscape health from 2002-2005, and once again disturbance from 2005-2008. The mortality sites were predominantly in the red and cyan portions of the image (middle). Future studies should look at sites within the cyan, as red is recovering and cyan has not yet recovered. Limiting sites to the disturbed area may yield more statistical significance with Landsat.

The lack of significance for EWDI, NDVI, and NDMI can also be attributed to poor spectral contrast between healthy and disturbed sites. Previous studies used large homogenous areas of bark beetle attack to quantify a spectral difference between mortality and non-mortality regions; indeed authors have warned that their methods for identifying and mapping bark beetle attack may not be applicable for areas that do not exhibit large areas of mortality (Healey *et al*., 2005). However, Landsat may sometimes detect small differences between mortality and non-mortality sites (using NDMI), and can map large regions undergoing stress (using EWDI and DI').

The negative relationship between DI', snowfall and precipitation intuitively describes decreasing disturbance with increasing moisture. However, high values in the tasseled cap wetness layer should theoretically result in lower DI' values because of increasing canopy moisture under the assumption that heavy years of rainfall result in lower disturbance levels. This was not the case in this study, as the year following lower tasseled cap wetness values also showed lower DI' values. Interpretation of the wetness layer can become complicated when taking into

consideration tree defoliation and increasing exposure of understory vegetation. The tasseled cap wetness layer uses a coefficient that emphasizes the SWIR band and is subtracted from the wetness value (Hais *et al.,* 2009). Therefore exposure to understory vegetation which has higher SWIR reflectance values than the forest canopy would result in a much lower wetness value even though the canopy may not be defoliating from bark beetle infestation and only has a smaller % canopy cover. In Sequoia National Forest, tree defoliation from bark beetles *did not* make a significant contribution to canopy openings, and therefore a true decrease in wetness in the canopy instead of increased exposure to understory vegetation is interpreted from these findings. This brings into question the role that drought may play in bark beetle infestation, and if nutrient loadings may better predict infestation than moisture content of the forest canopy.

The Landsat DI' Additive Color Logic Map (Figure 7) shows different areas of stress from the ASTER map (Figure 4a) due to the difference in the bands used. The cyan region in Landsat represents areas disturbed between 2002-2005 and areas that have not yet recovered by 2008, whereas the ASTER image marks areas experiencing stress between 2007-2008. However, it is important to note that both images display locations for further research. The Landsat color logic scene should be used for areas of current bark beetle damage, and the ASTER RVI scene for possible future bark beetle outbreaks. MODIS also shows promising results in identifying larger areas of possible bark beetle infestation.

CONCLUSION

Bark beetle mortality exhibits high ground level spatial heterogeneity in Sequoia National Park. It is recommended that high resolution satellite images for individual tree classification be used instead of 15 meter resolution. Further research is necessary to determine methods for remote detection of green attack in bark beetle outbreaks. If land managers can accurately detect the green attack stage, they can increase preemptive measures to reduce overall mortality from an outbreak.

Aerial detection surveys using large polygons group scattered infected stands with their healthy counterparts, causing mortality saturation to decline sharply. It is imperative that smaller, more accurate polygons with high mortality saturation be used to ensure best results, especially in areas of increased spatial heterogeneity. Future analyses should focus on the small polygons from the aerial surveys as well as locating large areas of dead trees to better identify the red-attack stage using satellites.

Satellite vegetation indices such as NDMI, RVI and DI show promising results for detecting stress, which is a primary precursor to bark-beetle infestation. These indices could be used to predict possible spread of bark beetles in the future. Low resolution MODIS images are capable of detecting areas for further research, whereupon higher resolution satellites may be used. Ground truthing and multiple index analyses remain invaluable for classification of bark beetle mortality sites. The soil nutrient potassium [K^+] should be investigated during future bark-beetle studies for the potential to explain the susceptibility of one area versus another.

ACKNOWLEDGMENTS

We gratefully acknowledge the efforts of our science advisor Cindy Schmidt and our mentor Dr. Jay Skiles. We also thank Nate Stephenson of the USGS and Lisa Fischer of the Forest Service for their generous time and insight into the project. We also thank Casey Teske and Brad Lobitz for their help with remote sensing.

APPENDIX A

Appendix A: Satellite indices in statistical analysis - Gray: Not Applicable, Purple: Marginaly Significant, Green: Significant

	Years					
Index	2003	2004	2005	2006	2007	2008
EWDI			t = 0.76, p = 0.46	t = 0.42, p = 0.68	t = 1.09, p = 0.29	t = 0.07, p = 0.94
NDVI	t = 0.99, p = 0.33	t = 0.96, p = 0.34	t = 1.53, p = 0.14	t = 1.15, p = 0.26	t = 1.46, p = 0.21	t = 1.13, p = 0.27
NDMI	t = 0.21, p = 0.83	t = 0.21, p = 0.83	t = 0.73, p = 0.47	t = 0.95, p = 0.35	t = 0.37, p = 0.72	t = 0.97, p = 0.34
Landsat DI	t = 0.12, p = 0.90	t = 0.56, p = 0.30	t = 1.42, p = 0.17	t = 0.62, p = 0.54	t = 0.38, p = 0.71	t = 0.74, p = 0.46
MODIS DI	t = 1.22, p = 0.24	t = 1.37, p = 0.19	t = 1.78, p = 0.10	t = 2.81, p = 0.01	t = 2.02, p = 0.06	t = 2.77, p = 0.02
RVI						t = 0.818, p = 0.56

REFERENCES

Amman, G. W., and Cole, W. E., 1983. Mountain pine beetle dynamics in lodgepole pine forests part II: Population dynamics, Technical Report. INT- 145 (p. 59), *USDA For. Serv. Gen*.

Ballard, R. G., Walsh, M. A., and Cole, W. E., 1982. Blue-stain fungi in xylem of lodgepole pine: A light microscope study on extent of hyphal distribution, *Canadian Journal of Botany*, 60, 2334– 2341.

British Columbia Ministry of Forests, 1995. Bark beetle management guidebook, *Forest Practices Code*, Victoria, BC' Forest Practices Branch. 45 pp.

Carroll, A. L., and Safranyik, L., 2004. The bionomics of the mountain pine beetle in lodgepole pine forests: Establishing a context, In T. L. Shore, J. E. Brooks, and J. E. Stone (Eds.), *Mountain Pine Beetle Symposium:* Challenges 164 M.A.

Carroll, A.L., Taylor, S.W., Régnière, J., Safranyik, L., 2004. Effects of climate change on range expansion by the mountain pine beetle in British Columbia, In T. L. Shore, J. E. Brooks, and J. E. Stone, (Eds.), *Mountain Pine Beetle Symposium: Challenges and Solutions*, 30–31 October 2003, Kelowna, British Columbia, Canada. Natural Resources Canada, Canadian Forest Service, Pacific Forestry Centre, Victoria, British Columbia, Information Report BC-X-399, pp. 223–232, 298.

Chander, G., and Markham, B., 2003. Revised Landsat-5 TM Radiometric Calibration Procedures and Post-calibration Dynamic Ranges, *IEEE Transactions on Geoscience and Remote Sensing*, 41(11): 2674-2677.

Crist, E. P. and R. J. Kauth, 1986. The tasseled cap de-mystified, *Photogrammetric Engineering & Remote Sensing*, 52(1): 81-86.

D'Antoni, H., Rothschild, L., Schultz, C., Burgess, S., and Skiles, J.W., 2007. Extreme environments in the forests of Ushuaia, Argentina, *Geophysical Research Letters*, 32: 1-5.

DeMars, C. J., Roettgering, B.H., 1982. Western Pine Beetle, Forest Insect & Disease Leaflet, *U.S.D.A. Forest Service*, http://na.fs.fed.us/spfo/pubs/fidls/we_pine_beetle/wpb.htm.

Desert Research Institute. Western Regional Climate Center, http://www.wrcc.dri.edu/index.html.

Elvidge C.D., D. Yuan, R.D. Weerackoon, and R.S. Lunneta, 1995. Relative radiometric normalization of Landsat Multispectral Scanner (MSS) data using an automatic scattergram-controlled regression, *Photogrammetric Engineering and Remote Sensing*, 61(10):1255-1260.

Ericsson, T., and M. Kähr, 1993. Growth and nutrition of birch seedlings in relation to potassium supply rate, *Trees-Structure and Function*, *7*(2), 78–85.

Franklin, S.E., L.M. Moskal, M. Lavigne and K. Pugh, 2000. Interpretation and classification of partially harvested forest stands in the Fundy model forest using multitemporal Landsat TM digital data, *Canadian Journal of Remote Sensing*, 26: pp. 318–333.

Hais, M., Jonasova, M., Langhammer, J., and Kucera, T., 2009. Comparison of two types of forest disturbance using multitemporal Landsat TM/ETM+ imagery and field vegetation data, *Remote Sensing of Environment, 113*: 835-845.

Healey, S., Cohen, W.B., Zhiqiang, W., Krankina, O.N., 2005. Comparison of Tasseled Cap-based Landsat data structures for use in forest disturbance detection, *Remote Sensing of Environment*, 97: 301-310.

Henigman, J., Ebata, T., Allen, E., and Pollard, A. (Eds.), 1999. Field guide to forest damage in British Columbia, Victoria, BC, British Columbia Ministry of Forests.

Hill, J. B., Poop, H. W., and Grove Jr., A. R., 1967. Botany: A textbook for colleges (4th edition), Toronto, ON' McGraw-Hill Book Co., 614 pp.

Jackson, T.J., Chen, D., Cosh, M., Li, F., Anderson, M., and Walthall, C., 2004. Vegetation water content mapping using Landsat data derived normalized difference water index for corn and soybeans, *Remote Sensing of Environment,* 92: pp. 475–482.

Jin, S., and Sader, S.A., 2005. Comparison of time series tasseled cap wetness and the normalized difference moisture index in detecting forest disturbances, *Remote Sensing of Environment, 94:* 364-372.

Keeley, J. E., and T. W. McGinnis, 2007. Impact of prescribed fire and other factors on cheatgrass persistence in a Sierra Nevada ponderosa pine forest, *International Journal of Wildland Fire*, *16*(1), 96.

Kilgore, B.M., 1973. The ecological role of Fire in Sierran Conifer Forests: Its Application to National Park Management, *Journal of Quaternary Research, 3*(3).

Matsushita, B., Yang, W., Chen, J., Onda, Y., and Qiu, G., 2007. Sensitivity of the Enhanced Vegetation Index (EVI) and Normalized Difference Vegetation Index (NDVI) to Topographic Effects: A Case Study in High-Density Cypress Forest, *Sensors,* 7, 2636-2651

Mildrexler, D.J., Zhao, M., Heinsh, F.A., Running, S.W., 2007. A New Satellite-Based Methodology for Continental Scale Disturbance Detection, *Ecological Applications*, 17(1): 235-250.

Minnich, R.A., and Padgett, P.E., 2003. Geology, climate, and vegetation of the Sierra Nevada and the mixed-conifer zone: An introduction to the ecosystem, *Developments in Environmental Science*, 2, 1-31.

National Park Service, 2009. NPS Data Store, http://science.nature.nps.gov/nrdata/index.cfm.

Reid, R. W., 1961. Moisture changes in lodgepole pine before and after attack by the mountain pine beetle, *Forestry Chronicle*, 368–375, http://www.for.gov.bc.ca/tasb/legsregs/fpc/fpcguide/beetle/betletoc.htm.

Safranyik, L., Shrimpton, D. M., and Whitney, H. S., 1974. Management of lodgepole pine to reduce losses from the mountain pine beetle, *Forestry Technical Report,* Vol. 1, Victoria, BC: Government of Canada.

Safranyik, L., and Carroll, A.L., 2006. The biology and epidemiology of the mountain pine beetle in lodgepole pine forests, In: Safranyik, L.,Wilson, B., (Eds.), *The Mountain Pine Beetle: A Synthesis of Biology, Management, and Impacts on Lodgepole Pine,* Natural Resources Canada, Canadian Forest Service, Victoria, British Columbia. pp. 3–66.

Samman, S., and Logan, J. (Eds.), 2000. Assessment and response to bark beetle outbreaks in the Rocky Mountain area, *Report to Congress from Forest Health Protection*, Washington Office, Forest Service, U.S. Department of Agriculture, Gen. Tech. Rep. RMRS-GTR-62, U.S. Department of Agriculture, Forest Service, Rocky Mountain Research Station, Ogden, UT, 46 pp.

Samuel Roberts Foundation, 2004. Don't overlook role of potassium, www.noble.org/Ag/Soils/RoleOfPotassium/

Short, N. M., 2005. Vegetation Applications: Agriculture, Forestry, and Ecology, *General Principles for Recognizing Vegetation,* URL: http://www.fas.org/irp/imint/docs/rst/Sect3/Sect3_1.html, Earth Observing System Goddard Program Office, Greenbelt, Maryland (last date accessed: 23 July 2009).

Skakun, R.S., Wulder, M.A., Franklin, S.E., 2003. Sensitivity of the thematic mapper enhanced wetness difference index to detect mountain pine beetle red-attack damage, *Remote Sensing of Environment*, 86, 433-443.

Thorne, J.H., Morgan, B.J., and Kennedy, J.A., 2008. Vegetation Change over Sixty Years in the Central Sierra Nevada, California, *Madrono*, 55(3), 223-237.

USDA Forest Service, 2009. Forest Health Technology Enterprise Team.
http://www.fs.fed.us/foresthealth/technology/gis.shtml.
http://www.fs.fed.us/r5/rsl/clearinghouse/gis-download.shtml#r5
http://www.fs.fed.us/r5/spf/fhp/fhm/aerial/

Van Mantgem, P.J., and Stephenson, N.L., 2007. Apparent climatically induced increase of tree mortality rates in a temperate forest, *Ecology Letters*, 10, 909-916.

Westfall, J., 2005. Summary of forest health conditions in British Columbia, Forest Practices Branch, Victoria, BC, British Columbia Ministry of Forests, 49 pp.

Wulder, M.A., 2006. Surveying mountain pine beetle damage of forests: A review of remote sensing opportunities, *Forest Ecology and Management,* 221: 27–41.